Clays and Clay Minerals, Vol. 39, No. 2, 184–190, 1991.

PRACTICAL NOTES CONCERNING THE INDEXING OF X-RAY POWDER DIFFRACTION PATTERNS OF CLAY MINERALS

S. W. BAILEY

Department of Geology and Geophysics, University of Wisconsin–Madison
Madison, Wisconsin 53706

Abstract—Hydrous phyllosilicate minerals exhibit many variations in unit-cell shape and symmetry, distortion due to cation ordering, polytypic repeats along Z, and lateral modulations that can affect the ease of indexing of X-ray powder diffraction patterns. In indexing the patterns of monoclinic and triclinic hydrous phyllosilicates it is important that the indices of all overlapping but nonequivalent lines be listed and used in the indexing program, with weights assigned according to their multiplicities. Deviations from orthogonal unit-cell geometry show up by a broadening or a splitting of nearly superimposed lines, as occurs also if the observed β angle differs from that produced by a layer shift of ideal magnitude (e.g., $a/3$). Observed powder intensities should be correlated with those expected from the structure, and an index should not be assigned solely on the basis of the calculated d-value that is closest to that observed. Assigned indices should not violate space group extinctions. Multilayer structures show up in reflections of type $k \neq 3n$ for C-centered unit cells, not in $00l$ reflections.

Key Words—Chlorite, Crystal structure, Indexing, Kaolinite, Mica, Modulated structures, Ordering, X-ray powder diffraction.

INTRODUCTION

To obtain correct indexing solutions of X-ray powder diffraction (XRD) patterns from hydrous phyllosilicate minerals, the structural variations that are possible in these minerals must be understood. The literature contains many examples of powder patterns of phyllosilicates that are indexed incorrectly, including some by the author. The purpose of the present paper is to present examples of structural variations that can cause indexing problems and to give suggestions for solving these problems.

Several assumptions are made in this paper.

1. Only hydrous phyllosilicate minerals are involved.
2. Each sample is pure; no extraneous lines due to impurities are present in the XRD patterns.
3. The powder particles are sufficiently small and randomly oriented so that the entire XRD pattern is recorded with smooth diffraction lines that have their proper intensities.
4. The stacking of layers is regular, and the samples are well enough crystallized to give a sufficient number of sharp diffraction lines to allow successful indexing of the powder patterns.
5. The reader has access to a computer indexing program similar to that of Appleman and Evans (1973). The similarity of the structural motifs in hydrous phyllosilicates makes it easy to obtain approximate unit-cell dimensions from the XRD patterns. Thus, it is not necessary to use an automatic indexing program, in which the pattern is treated as always triclinic or as based on some assumed symmetry.
6. Powder diffractograms or Debye-Scherrer XRD patterns are used, rather than oblique texture electron diffraction patterns.

UNIT-CELL SHAPE VS. SYMMETRY

The shape of a unit cell is an expression of the lattice geometry and is not necessarily directly related to its symmetry, which relates the positions and identities of the atoms to one another within the unit cells. For example, most chlorites have triclinic symmetry, but many are based on orthorhombic- or monoclinic-shaped unit cells; even the triclinic-shaped unit cells of the most common chlorites deviate from monoclinic geometry by only 0.5°. By definition, monoclinic symmetry allows one interaxial crystallographic angle (taken here to be β) to take any value, including 90°. Likewise for triclinic symmetry, all three interaxial angles may have any value, including 90°. In many computer indexing programs a starting "symmetry" must be assumed, but this term usually means the shape of the unit cell because the assumption controls the axial repeats and interaxial angles that may be varied during the computer run. The extinction conditions limiting the possible reflections may or may not be included.

Hydrous phyllosilicates can have hexagonal, trigonal, rhombohedral, orthorhombic, monoclinic, and triclinic symmetries. Hexagonal and trigonal cells are based on hexagonal-shaped lattices with three X-axes 120° apart and normal to Z; they differ by the presence of 6-fold or 3-fold axes, respectively, parallel to crystallographic Z. Rhombohedral crystals also have 3-fold axes parallel to Z of the hexagonal setting, but that Z is not normal to the three rhombohedral X-axes.

Copyright © 1991, The Clay Minerals Society

https://doi.org/10.1346/CCMN.1991.0390210 Published online by Cambridge University Press

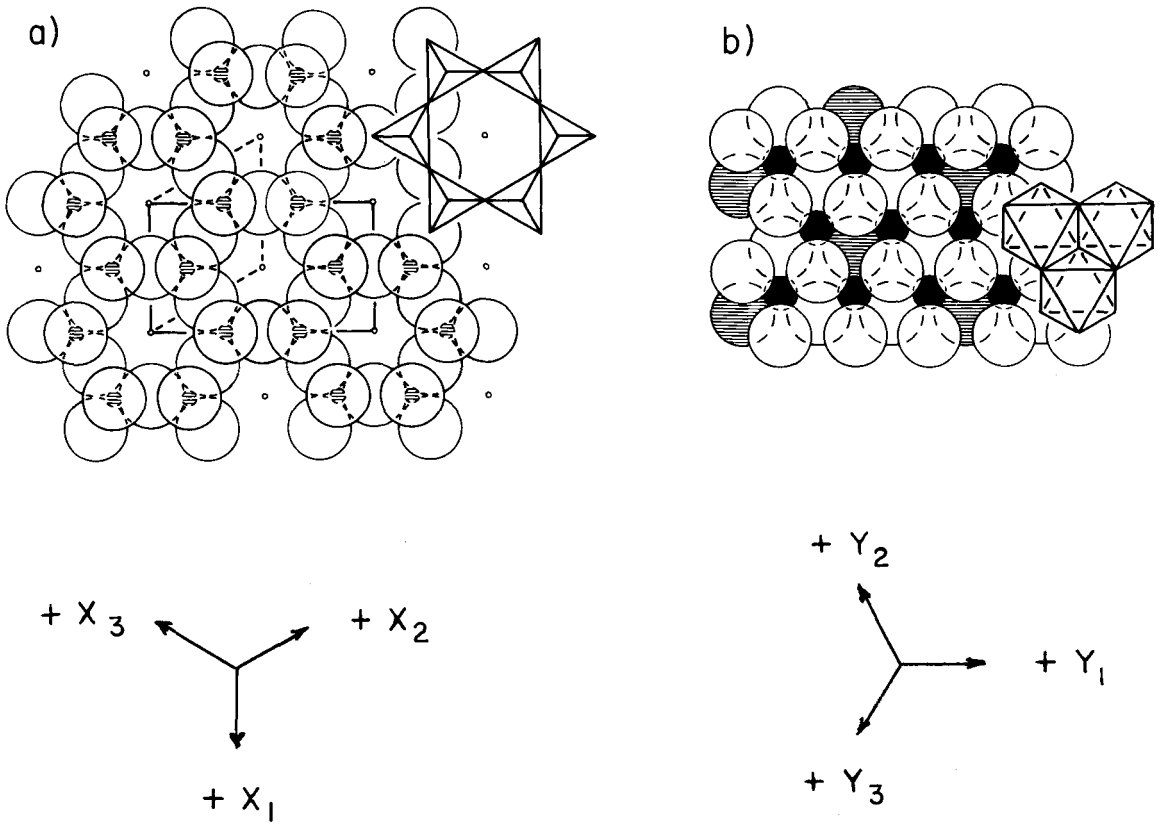


Figure 1. (a) Two alternative unit cells connecting lattice points (small circles) for the tetrahedral sheet of a phyllosilicate structure. Hexagonal-shaped cell (dashed) is primitive; orthohexagonal cell (solid line) is *C*-centered. (b) Octahedral sheet of a 1:1 phyllosilicate. All cations (solid) and anions (open and ruled) repeat at intervals of $b/3$ along the three possible orthohexagonal *Y*-axes inclined at 120° to each other.

Rhombohedral patterns may be indexed on hexagonal-shaped cells, however, but then reveal their rhombohedral nature by systematic absences. All reflections present will have *hkil* indices that obey either the obverse or reverse orientations of the rhombohedral unit cell, namely $(-h + k + l) = 3n$ or $(h - k + l) = 3n$.

Working with hexagonal indices *hkil* and rhombohedral indices *pqr* can be difficult. Common practice, therefore, is to index the XRD patterns of hydrous phyllosilicate minerals by using an orthohexagonal cell, rather than either a hexagonal- or rhombohedral-shaped cell. An orthohexagonal cell is defined with the *Y*-axis at 90° to one of the three *X*-axes, all taken as normal to *Z*, and with $b = a\sqrt{3}$ (Figure 1a). This orthohexagonal cell is *C*-centered and has twice the volume of the corresponding primitive cell based on hexagonal- or rhombohedral-shaped geometry. The smallest primitive unit cell contains one formula unit of atoms for a 1-layer phyllosilicate structure, whereas a *C*-centered cell contains two formula units for a 1-layer structure. An international agreement exists (Bailey, 1977) that all mineral compositions should be expressed in terms of formula units, not in terms of atoms per cell or half cell. The latter are variable with the cell shape and with the number of layers in the *c*-repeat.

For ease of comparison, all *hkl* indices in this paper will be expressed in terms of a unit cell that has a *C*-centered 5 Å × 9 Å base. The actual symmetry can be primitive, however, and hexagonal- or rhombohedral-shaped cells can be used in some cases. The justification for indexing all hydrous phyllosilicate minerals as *C*-centered is that exceptions to *C*-centering for an orthohexagonal cell are limited. For example, the Ba- and S-rich brittle mica anandite does not have *C*-centering. Cation and anion ordering in anandite creates a coordination group around the origin (0,0,0) of the cell that is different in composition and size than the group around the center of the *XY* base (½,½,0). As a result, reflections occur that violate the *C*-centering systematic absences of type $(h + k) = 2n$ (Filut *et al.*, 1985). Another example is the primitive form of minnesotaite, which has a modulated ribbon-like structure and is more Mg-rich than *C*-centered minnesotaite (Guggenheim and Eggleton, 1986). In both of these exceptions, however, those reflections that violate *C*-centering are too weak to observe on XRD

https://doi.org/10.1346/CCMN.1991.0390210 Published online by Cambridge University Press

powder patterns; they require the use of single crystals or electron diffraction techniques for resolution of the true symmetry. A published pattern of a hydrous phyllosilicate mineral based on a 5 Å × 9 Å unit cell that lists mixed even and odd h and k values, such as $21l$, is thus a clear indication of incorrect indexing unless proof is given that primitive symmetry exits. Modulated structures (to be discussed below) can lead to more complex unit cells (Guggenheim and Eggleton, 1988). For example, bementite is based on a primitive cell that does not have a 5 Å × 9 Å base. Ganophyllite, eggletonite, and bannisterite are based on A-centered cells.

LINE MULTIPLICITIES

Except for oblique texture patterns, all reflections of the same d-value will superimpose on the powder pattern, and the resulting line will have a multiplicity n that specifies the number of superimposed reflections. Thus, the 001 line has a multiplicity of $n = 2$ due to superposition of the 001 and 00$\bar{1}$ reflections. More importantly, because all hydrous phyllosilicates are based on a pseudohexagonal structure and most are close to the orthohexagonal lattice geometry of $b \approx a\sqrt{3}$, reflections of type $20l$ will superimpose or nearly superimpose on reflections of type $13l$ and $1\bar{3}l$ (plus Friedel equivalents). All of these reflections are *equivalent* in hexagonal or orthorhombic symmetry but not in lower symmetries. Thus, information may be lost about the intensities of the individual reflections that are important for determining the true symmetry. These lines (of the class $2h0l$, $h3hl$, and $h3\bar{h}l$) are the most intense on the powder patterns of hydrous phyllosilicates, except for certain mica polytypes.

In indexing the patterns of monoclinic and triclinic hydrous phyllosilicates it is important that the indices of all overlapping but nonequivalent lines be listed and used in the indexing program. For example, if only $20l$ indices are used for the strongest $k = 3n$ lines, an inaccurate value of the b repeat may result because of the paucity of indices with $k \neq 0$. Instead, for a line composed of superimposed non-Friedel reflections, several entries should be listed with different indices but the same d-value. Each entry should be weighted according to its multiplicity if the intensities of the individual reflections are about the same (see discussion below). Thus, for a monoclinic phyllosilicate mineral based on an orthohexagonal-shaped cell, $13l$ ($n = 4$) should have twice the weight of $20l$ ($n = 2$). For broad lines due to incipient separation of the lines (see below), slightly different d-values can be used for the lines involved.

LINE INTENSITIES

The intensity of an individual reflection in an XRD pattern is related to the position of each atom within the unit cell, the number of electrons associated with each atom, thermal vibration, and the diffraction angle. For hydrous phyllosilicate minerals all octahedral cations and anions repeat at intervals of $b/3$ along the three pseudohexagonal Y-directions (Figure 1b). Thus, these atoms scatter X-rays in phase only for reflections where $k = 3n$, and these lines are usually the most intense on the pattern. Basal oxygen atoms and mica interlayer cations contribute to all reflections, but they are the only contributors to reflections with $k \neq 3n$ for an undistorted structure. Hence, the lines with $k \neq 3n$ are generally less intense. Because of the pseudohexagonal nature of the structure of hydrous phyllosilicates, "triplets" of superimposed reflections (actually, $n = 6$) exist that have identical or nearly identical intensities and d-values. Examples of such "triplets" include reflections in the class $20l$, $13l$, and $1\bar{3}l$ (plus Friedel equivalents) for $k = 3n$ and $02l$, $11l$, and $1\bar{1}l$ (plus Friedel equivalents) for $k \neq 3n$. The l values within each "triplet" set may or may not be identical and will depend on the shape of the unit cell (see below). Despite their superposition, the similarity in intensities within the triplet set allows each reflection to be weighted according to its multiplicity during cell parameter refinement.

DEVIATIONS FROM ORTHOGONALITY

If $\beta = 90°$, the three pairs of reflections, $20l$ and $20\bar{l}$, $13l$ and $13\bar{l}$, $1\bar{3}l$ and $1\bar{3}\bar{l}$, plus their six Friedel equivalents superimpose precisely onto one line of multiplicity 12. Cation ordering may distort the structure away from orthogonality, thereby affecting the three interaxial angles (although in practice the γ angle commonly remains near 90°). If the distortion is small, the effect only broadens certain lines. With greater distortion, however, there is a separation of the lines that would superimpose with orthogonal geometry. A nonorthogonal cell then must be assumed in the indexing program and, to facilitate convergence, an approximate value of the appropriate angle should be entered. This angle and its approximate value can be determined from the pattern by noting the indices affected ($h0l$ or $0kl$) and the amount of separation of the lines. Figure 2 illustrates the progression from sharp lines to broad lines to resolved doublets for different specimens of amesite and kellyite. In these examples only the β angle is distorted from 90°, and the affected indices are of type $20l$ and $13l$. A deviation of 0.6° from 90° in kellyite is sufficient to resolve the doublets at d-values <2.2 Å for FeKα radiation using a 114.6-mm diameter Debye-Scherrer camera; even greater resolution would be achieved with a diffractometer.

If adjacent layers are shifted to give a monoclinic-shaped unit cell, e.g., by the layer stacking vector $-a/3$ found in $1M$ micas, a diffraction line that would have $n = 12$ for an orthogonal cell splits into two lines of $n = 6$ each. One line is of index $20\bar{l}$ and is superposed by reflections of index $13(l - 1)$ and $1\bar{3}(l - 1)$ plus their three Friedel equivalents ($n = 6$) for a $1M$ mica.

https://doi.org/10.1346/CCMN.1991.0390210 Published online by Cambridge University Press

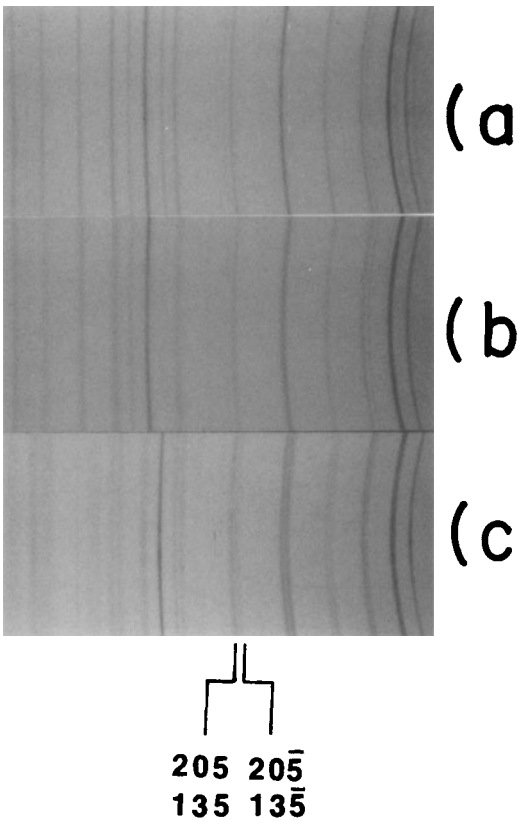


Figure 2. Change from sharp lines (a) to slightly broadened lines (b) to resolved doublets (c) as β angle progressively deviates from 90°. All X-ray powder diffraction patterns taken in a 114.6-mm diameter Gandolfi camera with graphite-monochromatized FeKα radiation. (a) amesite-6R_1, Antarctica, $\beta = 90°$. (b) amesite-6R_2, Ural Mtns., U.S.S.R., $\beta = 90.2°$. (c) kellyite-2H_2, Bald Knob, North Carolina, $\beta = 90.6°$.

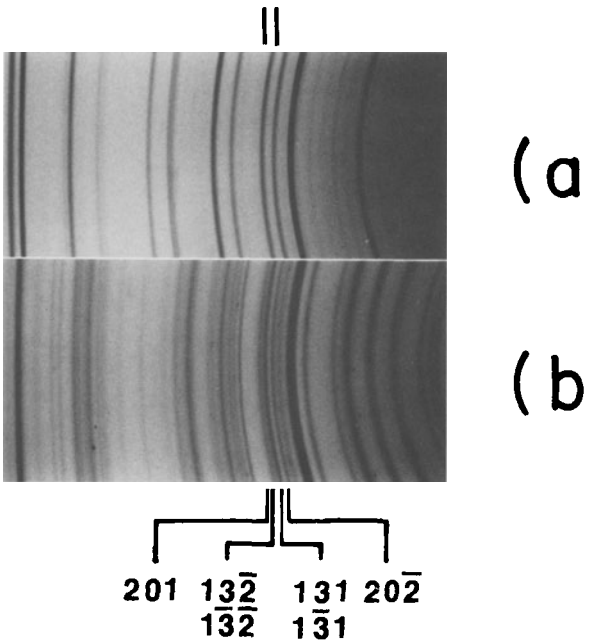


Figure 3. Splitting of superimposed lines (a) into doublets (b) when $\beta_{obs} > \beta_{ideal}$. (a) preiswerkite-2$M_1$ from Penninic Alps, Switzerland ($\beta_{obs} = \beta_{ideal}$). (b) muscovite-1$M$ from Fountain Fm near Commerce City, Colorado ($\beta_{obs} > \beta_{ideal}$ by 1.5°). Debye-Scherrer camera of 114.6-mm diameter with graphite-monochromatized FeKα radiation.

For example, 20$\bar{3}$ is superimposed by 132 and 1$\bar{3}$2, etc. The second line is of index 20l plus 13($\overline{l+1}$) and 1$\bar{3}$($\overline{l+1}$) and the three Friedel equivalents ($n = 6$). For example, 203 is superimposed by 13$\bar{4}$ and 1$\overline{34}$. The general case for 1M and 2M_1 micas is expressed as 2$h0l$ superimposes on $h3h(\bar{l} - h)$ and $h3\bar{h}(\bar{l} - h)$ plus the Friedel equivalents $2\bar{h}0l$, $\bar{h}3\bar{h}(l + h)$, and $\bar{h}3h(l + h)$. The amount of separation of the two lines is a function of the magnitude of the deviation of β from 90°, and the least-square routine in the refinement program will vary the β angle to achieve the best fit of the observed and calculated d-values or θ-angles. The amount of separation is large for a 1M mica ($\beta = 100°$); e.g., for lepidolite-1M d(20$\bar{2}$) = 2.48 Å and d(202) = 2.13 Å.

Structural distortion due to cation ordering may cause the resultant β angle to be larger or smaller than the ideal β angle given by an exact layer shift of $-a/3$ in the formula $\arccos(-a/3c) = \beta_{ideal}$. A deviation of ±0.2° from ideal is sufficient to split superimposed "triplets" ($n = 6$) at high angles. This deviation produces doublets in which one line is about twice as intense as the other (due to different multiplicities). Assuming that the cell axes are chosen so that the resultant layer shift is along $-X$, the doublet line 20$\bar{l}$ will have a larger d-value (but about half of the intensity) than line 13($l - 1$) + 1$\bar{3}$($l - 1$) for the usual case where $\beta_{resultant} > \beta_{ideal}$. Conversely, doublet line 20l will have a smaller d-value than line 13($\bar{l} + 1$) + 1$\bar{3}$($\bar{l} + 1$) (but about half of its intensity). Examples of both types of indices are illustrated for muscovite-1M in Figure 3. The splitting into doublets here is due to the octahedral ordering pattern in which the vacant M1 site is larger than the Al-rich M2 sites. This causes β_{obs} to be 1.5° greater than β_{ideal}. The splitting is much smaller in muscovite-2M_1.

In some samples a deviation of an angle from 90° is indicated only by a larger than normal deviation of observed and calculated d-values for a few lines if a 90° angle is assumed. For the di, trioctahedral chlorite sudoite, for example, the calculated d-values based on a monoclinic-shaped cell differ from the observed values by more than 3σ for the 1$\bar{3}$5, 1$\bar{3}$6, and 137 reflections (Fransolet and Bourguignon, 1978; Lin and Bailey, 1985). Observed versus calculated d-values for these indices were reported as 1.995 vs. 1.987 Å, 1.816 vs. 1.812 Å, and 1.549 vs. 1.553 Å, respectively. A single crystal study suggested the true symmetry is triclinic, and successful indexing of the powder pattern was achieved only by proposing a triclinic-shaped cell with $\alpha = 90.5°$ (Bailey and Lister, 1989). This triclinic distortion also has the effect of creating resolved doublets from reflections such as 068 and 0$\bar{6}$8, which would be equivalent in monoclinic symmetry (Figure 4).

https://doi.org/10.1346/CCMN.1991.0390210 Published online by Cambridge University Press

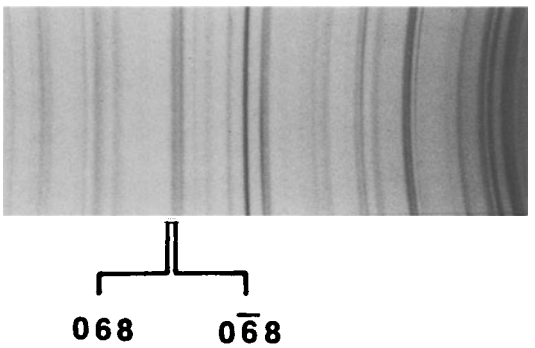


Figure 4. Splitting of lines that would be equivalent in monoclinic symmetry. Triclinic sudoite from Ottré, Belgium (α = 90.5°). Debye-Scherrer camera of 114.6-mm diameter with graphite-monochromatized FeKα radiation.

In kaolinite, the triclinic distortion is even larger, with $\alpha = 91.7°$, and this effect is combined with a larger-than-ideal β angle to create a powder pattern containing many resolved doublets and triplets (Bailey, 1980). Thus, 061 and $3\bar{3}\bar{2}$ are resolved from $0\bar{6}1$ and $33\bar{2}$, $20\bar{4}$ and $1\bar{3}3$, from 133, $11\bar{1}$ from $1\bar{1}\bar{1}$; $0\bar{2}1$ from 021, etc.

MULTILAYER STRUCTURES

The presence of a multilayer structure is indicated by additional *hkl* lines that cannot be indexed on the basis of a 1-layer repeat along *Z*. Because multilayer structures normally are caused by a particular stacking sequence of layers, the *c*-repeat is measured between planes of basal oxygen atoms within the layers that are truly identical. As mentioned above, the contributions of these atoms to the diffraction lines are best observed in reflections of index $k \neq 3n$ for which they alone contribute to the intensities without any contributions from the octahedral cations and anions. Thus, the additional lines for most multilayer polytypes will be indexed as 02*l*, 11*l*, 04*l*, 22*l*, etc., although in some minerals 20*l*, 13*l*, etc. may also be involved. The most visible additional lines will occur in the region of 4.5 to 3.0 Å. Tables of $k \neq 3n$ lines that identify the polytypes were given in the reviews of Bailey (1980, 1985, 1988a, 1988b). Figure 5 illustrates the 02*l* lines that identify the 6-layer structure of a synthetic serpentine.

The 00*l* type reflections never indicate the layer periodicities in multilayer polytypes. These reflections only record the layer thicknesses, such as 7 Å, 10 Å, 14 Å, and suborders thereof. Multiples of these values do not occur because adjacent layers normally have identical compositions, and their contributions to the intensities of multilayer 00*l* reflections exactly cancel out. Thus, a 3-layer mica will have a 10-Å line but not the 20-Å or 30-Å multiples.

If extra 00*l* lines are observed they must be due to one of the following causes:

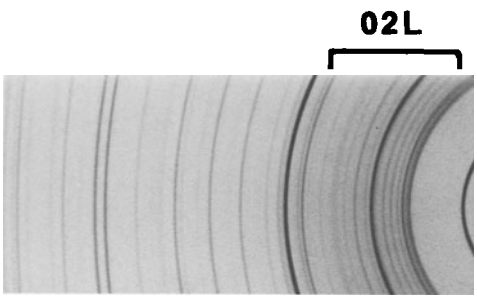


Figure 5. Sequence of 02*l* lines from $l = 3$ to $l = 13$ that identify the multilayer nature of a synthetic Mg-Ge serpentine. Filtered CuKα radiation, Debye-Scherrer camera of 114.6-mm diameter.

1. Regular interstratification of different layer types or interlayers so that adjacent unit structures either have different thicknesses or compositions. Under these circumstances a composite large spacing $d_{A(001)} + d_{B(001)}$ results, in addition to suborders of the large spacing, provided the regularity of interstratification is long-range in nature. Examples of these composite structures are corrensite and rectorite (Bailey, 1982). Gonyerite is a special case in which there is an interstratification of two layers that are structurally different as a result of modulation (Guggenheim and Eggleton, 1988).

2. Cation ordering between layers and consequent layer distortions so that adjacent layers or interlayers have different compositions or thicknesses. If the ordering is regular, a superlattice forms with a larger spacing than that of an individual layer. In addition to the regular interstratifications noted above, other examples include the hypothetical ordering of Na and Ca in alternate interlayers of mica, smectite, or vermiculite or a regular alternation of different amounts of layer substitutions and layer charges in adjacent layers.

3. The Renninger effect. Multiple reflections are usually limited to large particles. This effect is more commonly found in electron diffraction patterns. Multiple diffraction should not occur for small and randomly oriented particles within a powder. The use of a different wavelength is a test for the Renninger effect, as the extra reflections should then disappear.

4. Short-range interparticle diffraction at very small θ angles. These observed peaks are a function of particle size and do not record any large spacings within the particles. They do not exhibit suborder spacings.

IDEAL VS. REAL SYMMETRY

If all layers are identical and cation ordering does not occur, the particular stacking sequence of layers in a polytype produces an ideal symmetry (see Bailey, 1980, 1985, 1988a, 1988b). Most indexing programs require input on the systematic absences for the space group symmetry assumed for indexing. These systematic absences are in volume A of the *International*

https://doi.org/10.1346/CCMN.1991.0390210 Published online by Cambridge University Press

Tables for Crystallography (Hahn, 1983) and in several textbooks (e.g., Nuffield, 1966). The systematic absences may be bypassed, however, and the d- and θ-values may be calculated for all reflections. It is bad indexing procedure, however, to assign an index solely on the basis of the calculated d-value that is closest to that observed. The observed intensities should also be correlated with those expected from the structure. Intensity information may be available from published single-crystal structural refinements or from well-indexed powder patterns of similar minerals. If not previously published, the powder intensities can be calculated from the structure.

Many examples are known in which cation ordering, which probably takes place during the cooling of a crystal and after the layer-stacking sequence has been established, reduces the ideal symmetry to a lower (actual) subgroup symmetry. Examples of lower actual symmetries include those found in amesite-$2H_2$, kaolinite-1*Tc*, nacrite-2*M*, anandite-2*Or*, and margarite-$2M_1$ and in some specimens of lepidolite-1*M* and zinnwaldite-1*M*. The reduced symmetry has several possible effects on indexing. Weak powder lines may occur that violate the systematic absences of the ideal space group. The crystal system may be reduced, and the interaxial angles may change. All of these changes require some changes in input to the computer program used for indexing. The effect of change of interaxial angle was discussed above.

DERIVATION OF CELL PARAMETERS

Most computer programs for indexing also refine cell parameters by repeated cycles of least squares fit of calculated and observed d-values or θ-values. From experience it is possible to learn if a minimum reliability factor has been achieved for the quality of data used. Most programs provide a figure-of-merit to help make this judgment. Cycles should be repeated until no further changes in the calculated d-values or in the figure-of-merit occur; however, a false minimum may occur if some reflections are assigned fixed indices incorrectly.

Some programs require initial values of the cell parameters. For this purpose the d(00*l*) values give $c \sin\beta$, and the assumption of an approximate β angle for the polytype involved will give c. The b repeat can be derived from $b = 6 \times$ d(060) and the a repeat from $b = a\sqrt{3}$ as a first approximation.

Caution must be used if the b repeat is derived in this manner because "060" is usually a composite peak. Its multiplicity is $n = 6$. If b is indeed equal to $a\sqrt{3}$, the peak consists of three superimposed Friedel pairs of reflections, which for an orthogonal cell will be 060 + $0\bar{6}0$, $\bar{3}\bar{3}0$ + 330, and $3\bar{3}0$ + $\bar{3}30$. For a monoclinic- or triclinic-shaped cell due to layer shifts of $a/3$ or $b/3$, a certain 33*l* peak with $l \neq 0$ will superimpose on 060. For example, in 1*M* and $2M_1$ micas 06*hl* is superimposed by $3h3h(\bar{h} \pm l)$ and $3h3\bar{h}(\bar{h} \pm l)$ reflections. The composite peak gives the true b repeat only if the lattice has a $b = a\sqrt{3}$ relationship.

If the structure is distorted by cation ordering so that $b \neq a\sqrt{3}$, the 33*l* and $3\bar{3}l$ reflections shift relative to 060 to produce an asymmetric peak. Because all of the superimposed or nearly superimposed reflections have about the same intensities, the resultant peak is dominated by the 33*l* + $3\bar{3}l$ components. Thus, the composite, distorted peak is more a measure of the lateral repeats along the two directions at 120° to crystallographic *Y* than it is of the b repeat.

MODULATED STRUCTURES

Structural strain due to poor lateral misfit between a smaller Si-rich tetrahedral sheet and a larger octahedral sheet populated with cations the size of Mg, Fe, and Mn can be relieved by a regular modulation. In this modulation tetrahedra invert at regular intervals along *X*, *Y*, or both, and then relink their apices in some regular pattern. This creates a superlattice along *X* and/or *Y* that may or may not be an integral multiple of the planar lateral repeat (commensurate or incommensurate structures). The presence of the superlattice is indicated by extra spots (single crystal) or lines (powder) on the diffraction patterns or, in some minerals, by satellite spots adjacent to normal reflections (observed most easily by electron diffraction).

Reflections from superlattices commonly are too weak to be visible on powder patterns; however, modulation can be suspected for compositions of this type if the powder pattern cannot be indexed on the basis of an ideal non-modulated structure. High-resolution transmission electron microscope photographs have imaged the modulations in greenalite and minnesotaite, for example, which for many years were considered to be ferrous analogues of serpentine and talc, respectively, but for which the powder patterns could not be indexed on the basis of a single homogeneous planar structure (Guggenheim *et al.*, 1982; Guggenheim and Bailey, 1982; Guggenheim and Eggleton, 1986). Other examples of modulated phyllosilicates are caryopilite, antigorite, sepiolite, palygorskite, stilpnomelane, ganophyllite, and zussmanite (Guggenheim and Eggleton, 1987).

STACKING FAULTS

The presence of stacking faults in phyllosilicates affects indexing because the faults can broaden and shift the positions of powder peaks. In the extreme case, three-dimensional *hkl* peaks weaken and disappear within two-dimensional *hk* bands, in which no true repeat exists along *Z* for the basal oxygen atoms and no *l* index can be assigned. Good examples are the 02,11 and 04,22 bands in some forms of defect kaolinite (see, e.g., Brindley, 1980). If these defect kaolinite patterns are indexed on the basis of the re-

https://doi.org/10.1346/CCMN.1991.0390210 Published online by Cambridge University Press

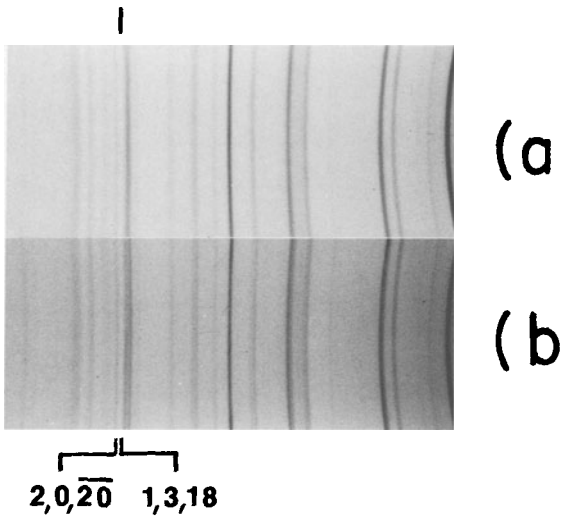


Figure 6. Change in positions of $k = 3n$ lines depending on whether layers are stacked in random (a) or regular (b) fashion. Cookeite from North Little Rock, Arkansas. Gandolfi camera of 114.6-mm diameter with graphite-monochromatized FeKα radiation.

maining three-dimensional reflections, the cell shape approaches monoclinic in contrast to the triclinic shape of the unit cell of well-crystallized kaolinite. This means that reflections of index $k = 3n$ change positions as a consequence of the regularity or irregularity of the stacking of adjacent layers. Figure 6 illustrates this effect for a 2-layer I*a* cookeite specimen based on the "*r*" structure of Mathieson and Walker (1954). In the vicinity of d = 1.3 Å the 13,18 and 20,$\bar{2}$0 lines are split into a doublet because $\beta_{\text{resultant}} \neq \beta_{\text{ideal}}$ for the regular stacking variant (Figure 6b). The lines coalesce for the randomly stacked example (Figure 6a), and this coalescence correlates with the loss of all $k \neq 3n$ lines. Moreover, the pattern in Figure 6b changes to that in Figure 6a upon severe grinding of the specimen. Even moderate grinding should therefore be avoided for the more sensitive trioctahedral chlorites and 1:1 structures.

Two-dimensional bands are very common in chlorite (e.g., see Bailey, 1988b), because several possibilities exist for positioning of adjacent layers to provide hydrogen bonds with the interlayer hydroxide sheet. This semi-random stacking of $\pm b/3$ shifts normally affects only reflections of index $k \neq 3n$; however, examples are known (Ib_d chlorites) of semi-random disorder affecting both $k = 3n$ and $k \neq 3n$ reflections. In this extreme case only the 00*l* reflections remain unaffected.

ACKNOWLEDGMENTS

This research was supported in part by National Science Foundation grant EAR-8614868 and in part by grant 17966-AC2-C from the Petroleum Research Fund, administered by the American Chemical Society. The manuscript has benefited from critical reviews by S. Guggenheim and M. L. Ross.

REFERENCES

Appleman, D. E. and Evans, H. T., Jr. (1973) U.S. Geological Survey Computer Contributions 20: *U.S. Natl. Tech. Inf. Serv. Doc.* **PB2-16188.**

Bailey, S. W. (1977) Report of the I.M.A.-I.U.Cr. Joint Committee on Nomenclature: *Amer. Mineral.* **62,** 411–415.

Bailey, S. W. (1980) Structures of layer silicates: in *Crystal Structures of Clay Minerals and their X-ray Identification,* G. W. Brindley and G. Brown, eds., Mineral. Soc., London, 1–123.

Bailey, S. W. (1982) Nomenclature for regular interstratifications: *Clay Miner.* **17,** 243–248.

Bailey, S. W. (1985) Classification and structures of the micas: in *Micas,* S. W. Bailey, ed., *Reviews in Mineralogy* **13,** Mineralogical Society of America, Washington, D.C., 1–12.

Bailey, S. W. (1988a) Polytypism of 1:1 layer silicates: in *Hydrous Phyllosilicates (Exclusive of Micas),* S. W. Bailey, ed., *Reviews in Mineralogy* **19,** Mineralogical Society of America, Washington, D.C., 9–27.

Bailey, S. W. (1988b) Chlorites: Structures and crystal chemistry: in *Hydrous Phyllosilicates (Exclusive of Micas),* S. W. Bailey, ed., *Reviews in Mineralogy* **19,** Mineralogical Society of America, Washington, D.C., 347–403.

Bailey, S. W. and Lister, J. (1989) Structures, compositions, and X-ray diffraction identification of dioctahedral chlorites: *Clays & Clay Minerals* **37,** 193–202.

Brindley, G. W. (1980) Order-disorder in clay mineral structures: in *Crystal Structures of Clay Minerals and their X-ray Identification,* G. W. Brindley and G. Brown, eds., Mineral Soc., London, 125–195.

Filut, M. A., Rule, A. C., and Bailey, S. W. (1985) Crystal structure refinement of anandite-2*Or,* a barium- and sulfur-bearing trioctahedral mica: *Amer. Mineral.* **70,** 1298–1308.

Fransolet, A.-M. and Bourguignon, P. (1978) (Di/trioctahedral chlorite in quartz veins from the Ardenne, Belgium: *Can. Mineral.* **16,** 365–373.

Guggenheim, S. and Bailey, S. W. (1982) The superlattice of minnesotaite: *Can. Mineral.* **20,** 579–584.

Guggenheim, S., Bailey, S. W., Eggleton, R. A., and Wilkes, P. (1982) Structural aspects of greenalite and related minerals: *Can. Mineral.* **20,** 1–18.

Guggenheim, S. and Eggleton, R. A. (1986) Structural modulations in Mg-rich and Fe-rich minnesotaite: *Can. Mineral.* **24,** 479–497.

Guggenheim, S. and Eggleton, R. A. (1987) Modulated 2:1 layer silicates: review, systematics, and predictions: *Amer. Mineral.* **72,** 724–738.

Guggenheim, S. and Eggleton, R. A. (1988) Crystal chemistry, classification, and identification of modulated layer silicates: in *Hydrous Phyllosilicates (Exclusive of Micas),* S. W. Bailey, ed., *Reviews in Mineralogy* **19,** Mineralogical Society of America, Washington, D.C., 672–725.

Hahn, T., ed. (1983) *International Tables for Crystallography, Vol. A, Space-group Symmetry:* Reidel, Dordrech, The Netherlands, 854 pp.

Lin, C.-Y. and Bailey, S. W. (1985) Structural data for sudoite: *Clays & Clay Minerals* **33,** 410–414.

Mathieson, A. McL. and Walker, G. F. (1954) Crystal structure of magnesium-vermiculite: *Amer. Mineral.* **39,** 231–255.

Nuffield, E. W. (1966) *X-ray Diffraction Methods:* Wiley, New York, 409 pp.

(Received 16 August 1990; accepted 25 September 1990; Ms. 2030)

https://doi.org/10.1346/CCMN.1991.0390210 Published online by Cambridge University Press